Alkyl Chain Ordering of Asymmetric Phosphatidylcholines Adsorbed at a Liquid−Liquid Interface

B. L. Smiley and G. L. Richmond*

Department of Chemistry, University of Oregon, Eugene, Oregon 97403

Received: April 27, 1998; In Final Form: November 3, 1998

Vibrational spectroscopic investigations of hydrocarbon chain ordering in phosphatidylcholines (PCs) adsorbed from aqueous solution to a carbon tetrachloride−water interface presented here examine on a molecular level the organization pertinent to the surface characteristics displayed by these films. In a series of saturated symmetric and asymmetric chain PCs, both symmetric PCs with 16 or fewer carbons per acyl chain and highly asymmetric PCs produced relatively disordered films at the liquid−liquid interface. The longest chain PCs studied, 1,2-distearoyl-*sn*-glycero-3-PC (C_{18}/C_{18}), 1-stearoyl-2-palmitoyl-*sn*-glycero-3-PC (C_{18}/C_{16}) and 1-palmitoyl-2-stearoyl-*sn*-glycero-3-PC (C_{16}/C_{18}), formed well-ordered layers at room temperature. The results can be explained in terms of enhanced chain−chain interactions among the longer, nearly symmetric hydrocarbon chains. Properties of the neat liquid−liquid interface that may influence the formation of these well-ordered two-dimensional phases are discussed.

Introduction

Surfactant monolayers adsorbed at oil−water interfaces in biological organisms are involved primarily in the formation and stabilization of emulsions that allow water-insoluble fats to be consumed and metabolized in an aqueous environment. The best known examples include bile salts secreted into the intestinal tract for the digestion of dietary fats[1] and plasma lipoproteins (PLs), which include chylomicrons from the small intestine and very low-density lipoproteins (VLDLs) produced by the liver.[2] PLs are the means by which digested fats are transported through the blood stream. They consist mostly of a triglyceride core surrounded and stabilized by a phospholipid monolayer composed primarily of phosphatidylcholines (PCs) and a small percentage of surface-adsorbed protein.[3] Proteins in the blood bind to the PL surface and begin to hydrolyze the triglyceride core and only a small fraction of the phospholipids such that the core volume shrinks and the surface monolayer begins to flatten and transform into bilayer structures.[4] The efficiency with which surface-adsorbed proteins are able to hydrolyze the triglyceride core has been shown to depend on the acyl chain composition of monolayer PCs.[5] Other than bulk thermodynamic properties, however, little is known on the molecular level about the organization of adsorbed PCs at a liquid−liquid interface that would lead to different metabolic effects observed as a function of hydrocarbon chain composition.

Interest in the commercial use of natural phosphatidylcholines (or lecithins) as emulsifiers, including their use in delivery of water-insoluble drugs[6] and in food preparations,[7] arises from the unusual natural surface properties of PCs.[8] The ability of PCs to form condensed, relatively stable monolayers at an oil−water interface in comparison to monolayers formed by other surfactants (e.g., phosphatidylserine, phosphatidylethanolamine, cholesterol, and oleic acid) is well recognized.[2,8] A surfactant's ability to form a liquid-condensed film at the oil−water surface is in fact considered prerequisite for the formation of a thermodynamically stable microemulsion.[1] The role of PCs as an essential component in lung surfactant monolayers has also been well recognized,[9] while PCs and other phospholipids in bilayer form (i.e., liposomes) are perpetually being studied as model cell membranes.[10] Our aim in the described work has been to shed further light on the molecular-level structure of PCs adsorbed at an oil (CCl_4)−water interface, looking specifically at ordering of the hydrocarbon chains.

The large majority of biological phospholipids contain two dissimilar hydrocarbon chains per molecule. The two chains may differ in length and degree of unsaturation such that a highly complex mixture of phospholipid structures is present in a particular bilayer membrane, allowing other structural elements such as integral membrane proteins, which are distributed asymmetrically across a bilayer, to be accommodated without disruption of bilayer integrity.[11] Despite the asymmetry typical of phospholipids in vivo, bilayer and particularly monolayer investigations aimed at understanding the structural organization and properties of these molecules have focused mostly on saturated, symmetric chain phospholipids, with some exceptions.[12,13] Little is therefore known about asymmetric chain phospholipids in bilayers, and even less is known about their monolayer properties.

In the bilayer state below the gel-to-liquid crystalline phase transition temperature, the packing arrangement adopted by a particular type of PC is largely determined by the amount of chain mismatch between two saturated hydrocarbon chains.[11] An intermediate degree of chain length mismatch, between that of well-ordered PC bilayers with high and low chain mismatch, actually produces the most disordered bilayer state of the hydrocarbon chains due to the nature of chain−chain interactions between opposing monolayers.[11] We expect adsorbed PCs in the absence of an opposing monolayer to exhibit distinctly different trends as a function of chain mismatch. Our measurements at the oil−water interface utilizing nonlinear optical vibrational spectroscopy to selectively probe the adsorbed layers indicate clear trends in chain ordering not anticipated based on available thermodynamic data.

* Corresponding author. E-mail: richmond@oregon.uoregon.edu. Fax: (541) 346-5859.

10.1021/jp982008p CCC: $18.00
Published on Web 01/09/1999

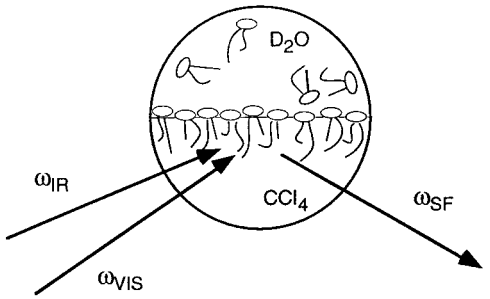

Figure 1. Schematic representation of VSFS from the CCl_4−water interface utilizing a total internal reflection geometry. ω_{vis} is incident on the liquid−liquid interface and ω_{SF} is emitted at their respective critical angles. PC layer formation occurred by adsorption from the top aqueous phase.

Theoretical Considerations

Vibrational Sum Frequency Spectroscopy. Vibrational sum frequency spectroscopy (VSFS) is a surface-specific nonlinear optical technique that has been widely applied in the study of molecular-level ordering at many types of gas, liquid, and solid interfaces, including buried interfaces.[14−17] Sum frequency generation, as a second-order process, is symmetry forbidden in isotropic media under the electric dipole approximation and is therefore allowed only at interfaces where the inversion symmetry is necessarily broken. Surface-specific information may therefore be gained using VSFS even at buried interfaces where adsorbed molecules are in equilibrium exchange with the surrounding bulk solutions.

Spatial and temporal overlap of two intense optical fields at frequencies ω_1 and ω_2 on a surface induces a polarization, P_{SF}, in the surface region at the sum frequency of the two fields, $\omega_{SF} = \omega_1 + \omega_2$. As given in eq 1, the induced polarization generates an electric field, E_{SF}, proportional to the product of the amplitudes of the incident electric fields, and to the second-order nonlinear susceptibility, $\vec{\vec{\chi}}^2$, of the surface region on which the fields are incident.

$$E_{SF} \propto P_{SF} = \vec{\vec{\chi}}^2 E_{vis} E_{IR} \tag{1}$$

In these experiments, the more intense field, $E(\omega_1) = E_{vis}$, is in the visible region and the second field, $E(\omega_2) = E_{IR}$, is tunable across the IR region of interest. The SF signal intensity is measured in reflection as shown schematically in Figure 1. The signal generated at the sum frequency, ω_{SF}, is resonantly enhanced due to an increased molecular polarizability when ω_{IR} is tuned across allowed molecular vibrational transitions. Our measurements are dominated by the resonant component of the second-order nonlinear susceptibility, $\vec{\vec{\chi}}_R^{(2)} = N\langle\alpha^{(2)}\rangle$, which is proportional to the molecular hyperpolarizability, $\alpha^{(2)}$, and the surface density, N, of interfacial molecules contributing to the sum frequency signal. An average is taken over the distribution of molecular orientations in the surface region as indicated by the brackets. Equation 2 describes the frequency dependence of α^2,

$$\alpha^{(2)} = \sum_n \frac{A_n}{\omega_n - \omega_{IR} - i\Gamma_n} \tag{2}$$

where, summing over all vibrational modes, ω_n is the frequency of the nth vibrational mode, Γ_n is the width of the transition, and A_n is an amplitude coefficient proportional to the product of the Raman and IR transition moments.[18] For a vibrational mode to be sum frequency active, A_n must be nonzero, which requires that both the Raman and IR transition moments are nonzero for the particular vibration. As ω_{IR} approaches the frequency of an allowed vibrational transition, $\alpha^{(2)}$ in eq 2 becomes very large and a relatively large sum frequency signal is generated from the interface. Judicious choice of polarization conditions for the ω_{vis} and ω_{IR} fields incident on the sample surface and selection of the polarization of the SF field measured using an analyzer allows SF active vibrational modes either normal to or in the plane of the surface to be separated. Data reported are for vibrational modes with a component normal to the interface plane. A total internal reflection geometry is used to obtain up to 2 orders of magnitude enhancement in the generated sum frequency signal reflected from the interface.[19,20]

Materials and Methods

Materials. Phosphatidylcholines of all chain permutations were obtained from Avanti Polar Lipids (Alabaster, AL) in powder form (purity greater than 99%) and used as received. The racemic mixture of DSPC, 99% purity, was obtained from Sigma Chemical Company (St. Louis, MO). Carbon tetrachloride (CCl_4), 99.9+%, HPLC grade, was from Sigma-Aldrich. Phosphate buffer, 10 mM, pH 7.0 prepared in deuterium oxide (D_2O), 99.9%, HPLC grade, either from Aldrich (Milwaukee, WI) or Cambridge Isotope Laboratories (Andover, MA) was used as the aqueous phase and for preparation of phospholipid stock solutions.

Sample Preparation. The sample cell and all glassware were soaked in Nochromix glass cleaner, rinsed in water from a Barnstead Nanopure filtration system, and dried in an oven prior to use. Phospholipid stock solutions were prepared at concentrations less than 1 mM by prewarming the powder in D_2O buffer to above the gel-to-liquid crystalline phase transition temperature, T_m, for the particular lipid, followed by bath sonication, also above T_m, for a time period at least sufficient to form a homogeneous solution. Following sonication, stock solutions were allowed to cool to room temperature before use. The sample cell was prepared with CCl_4 as the bottom phase and D_2O buffer as the top phase and allowed to sit for at least 2 h prior to addition of the phospholipid in order to allow any possible surface-active contaminants to adsorb at the liquid−liquid interface. The sample cell was recleaned and prepared again with fresh solutions if surface contamination was evident at the neat CCl_4−D_2O buffer interface. Phosphatidylcholine layers were then prepared at the CCl_4−aqueous interface as follows. (1) An injection of the PC stock solution was made into the bulk aqueous phase using a Hamilton syringe. (2) PC adsorption to the CCl_4−D_2O interface was allowed to occur overnight. (3) In general, a second injection from the same stock phospholipid solution was made following the overnight equilibration period. This second injection was made vigorously such that the partially formed PC interfacial layer was physically perturbed by the addition. The sample cell was allowed to sit for several hours following the second injection. The second injection was necessary to promote room temperature formation of a complete interfacial layer given that PCs, which are below their respective gel-to-liquid crystalline phase transition temperatures under ambient conditions, do not form complete layers from a single concentrated injection.[21] VSFS measurements were typically done the same day after the sample preparation was completed and on the same sample the following day. It was assumed that a stable interfacial structure was obtained when VSFS measurements did not indicate a substantial variation in the measured parameters beyond the normal error bar. For some of the PCs, particularly those found to be less well-ordered by

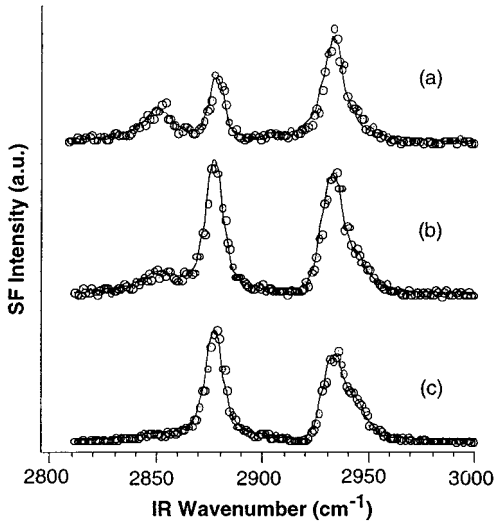

Figure 2. VSFS spectra for (a) MSPC (C_{14}/C_{18}), (b) PSPC (C_{16}/C_{18}), and (c) DSPC (C_{18}/C_{18}) adsorbed at the CCl_4−water interface shown as a function of IR wavenumber for S-polarized sum frequency S-polarized visible, and P-polarized IR fields. The aqueous phase was 10 mM phosphate buffer, pH 7.0, in D_2O.

VSFS, the second stock solution injection did not significantly affect chain ordering. Therefore, data for layers prepared by both single and double stock solution injections are included for these points. We do not assume that monolayers are necessarily formed by the PC molecules since it is possible that multilayer PC structures are produced at the interface.[22]

Vibrational Spectroscopy. The optical system used for VSFS measurements has been described previously.[23] Only a brief description is therefore given here. The visible field at 532 nm is generated by frequency-doubling a portion of the 1064 nm output of a Nd:YAG laser producing 12 ns pulses at 10 Hz. The 532 nm pulse energy used in these experiments was approximately 6.5 mJ. The other portion of the 1064 nm Nd:YAG output generates 1−2 mJ IR pulses tunable in the range 3.2−3.7 μm via a $LiNbO_3$ optical parametric oscillator. The laser system has a 6 cm^{-1} bandwidth. The 532 nm beam is directed at the sample surface at approximately its critical angle, as shown in Figure 1. The tunable IR beam is focused into the sample cell, overlaping the 532 nm sample spot centered on the interface. Small adjustments were then made to the incident angle of the visible beam to maximize the SF intensity measured in reflection. D_2O, rather than H_2O, is used as the aqueous phase to reduce absorption of the IR pulse energy by water at the sample interface, which can cause boiling.

Results and Discussion

Spectra from 1-myristoyl-2-stearoyl-*sn*-glycero-3-PC (MSPC), 1-palmitoyl-2-stearoyl-*sn*-glycero-3-PC (PSPC), and 1,2-distearoyl-*sn*-glycero-3-PC (DSPC) layers adsorbed at the CCl_4−D_2O interface for S-polarized sum frequency signal and S-polarized visible and P-polarized IR fields (i.e., SSP) are shown in Figure 2 as a function of the IR wavenumber. Close-packed layers were formed at the CCl_4−D_2O interface for these samples as evidenced by a complete relaxation of the meniscus between the two liquids, with the exception of the DSPC film, which displayed a small amount of residual surface curvature. Representative surface pressure measurements of similarly prepared samples indicated terminal surface pressures of approximately 42 mN/m in agreement with other studies.[24] The MSPC (C_{14}/C_{18}) spectrum in Figure 2a shows a prominent methylene symmetric stretch (CH_2-SS) peak centered at 2850 cm^{-1} next to the more narrow methyl symmetric stretch (CH_3-SS) peak at 2875 cm^{-1}.[17,25] These two peak assignments have been confirmed by recent studies on selectively deuterated surfactants.[17] A vibrational resonance peaked at approximately 2932 cm^{-1} is thought to include contributions from methylene asymmetric stretches (CH_2-AS), with the shoulder on the high energy side at approximately 2944 cm^{-1} assigned to a methyl Fermi resonance (CH_3-FR).[17,25] The broad structure centered at approximately 2905 cm^{-1} has been assigned to a methylene Fermi resonance.[17,25]

TABLE 1: Phosphatidylcholine Chain Ordering at the CCl_4−D_2O Interface

PC molecule (C_{sn-1}/C_{sn-2})	peak ratio	ΔC/CL	T_m (°C)[23]
SCPC (18:10)	0.56 ± 0.11	0.56	20
SLPC (18:12)	0.60 ± 0.14	0.44	18
SMPC (18:14)	0.80 ± 0.16	0.32	30
SPPC (18:16)	2.60 ± 0.78	0.21	44
DSPC (18:18)	4.59 ± 1.38	0.09	55
PLPC (16:12)	0.78 ± 0.16	0.37	10
PMPC (16:14)	0.93 ± 0.19	0.23	27
DPPC (16:16)	1.17 ± 0.24	0.10	41
PSPC (16:18)	3.08 ± 0.93	0.03	49
DMPC (14:14)	1.10 ± 0.22	0.12	23
MPPC (14:16)	0.83 ± 0.17	0.04	36
MSPC (14:18)	0.74 ± 0.15	0.16	40
DLPC (12:12)	1.30 ± 0.26	0.14	−1

The SSP polarization condition selects only sum frequency active vibrational modes with a component of the transition moment normal to the interface plane. In the SSP spectra, we use the area ratio of the CH_3-SS to the CH_2-SS to provide a relative measure of PC hydrocarbon chain ordering.[14] Other analyses, such as calculation of the terminal methyl group tilt angle, have been applied to VSFS spectra of a variety of surfactants adsorbed at an air−water interface in an effort to compare monolayer chain ordering but have been found relatively insensitive to changes in ordering particularly for chain tilt angles near normal to the interface.[14] The peak ratio method, which directly depends on intermolecular and intramolecular symmetries, was therefore expected to provide the most quantitative measure of chain conformation in our condensed interfacial layers of PCs. For very well-ordered layers with all-trans chain conformations, the CH_2-SS is symmetry forbidden in VSFS and is therefore absent.[26] As chain disorder in the film increases, the CH_2-SS becomes sum frequency active to a degree related to the degree of hydrocarbon chain disorder. However, since the CH_2-SS mode intensity should depend both on the number and relative orientations of the CH_2 groups present, any attempt to directly correlate the CH_2-SS peak intensity and the number of contributing oscillators is difficult. The CH_3-SS mode shows increased intensity with increased chain ordering as the fields couple to a less random and more upright orientation of the CH_3 symmetry axis. Consequently, the area ratio CH_3-SS/CH_2-SS becomes very large for well ordered chains and is small for disordered chains from a combined effect. The calculated ratio CH_3-SS/CH_2-SS is 0.74 ± 0.15 for MSPC (C_{14}/C_{18}) (Figure 2a), as determined from experiments on multiple samples. The prominent signal from the CH_2-SS mode indicates that this is a relatively disordered interfacial layer. In Figure 2b, a representative SSP spectrum for PSPC (C_{16}/C_{18}), which has two more methylene units in the sn-1 chain than MSPC, is shown with a much less prominent CH_2-SS mode and a strong CH_3-SS mode compared to MSPC. The spectrum for symmetric chain DSPC (C_{18}/C_{18}) shows little or no CH_2-SS. As given in Table 1, the calculated ratios for PSPC and DSPC are 3.08 ± 0.93 and 4.59 ± 1.38, respectively. The larger error inherent in the measure-

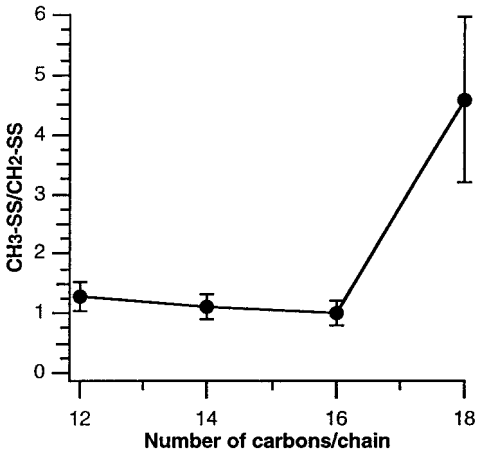

Figure 3. CH_3-SS/CH_2-SS peak area ratios, which provide a measure of the degree of hydrocarbon chain ordering, for VSFS peaks obtained from the symmetric chain PC layers as a function of the number of carbon atoms per alkyl chain.

ments for the more ordered layers stems from difficulty in determining the area of a very small CH_2-SS peak overlapping the tail of the CH_3-SS mode. Nevertheless, it is clear that the hydrocarbon chains of both PSPC and DSPC are extremely well-ordered with few gauche conformations, which on the basis of the strong CH_3-SS mode, likely are oriented near normal to the surface plane. This observation is consistent with increased chain−chain interactions expected for the longer alkyl chains, as has been observed in monolayers at the air−water interface.[12,13,24] All three PCs, in bilayer form, are below T_m in their respective gel states at room temperature,[27] and it has been reported that monolayer transition temperatures for PCs at the oil−water interface of emulsions are comparable to the well-established bilayer values.[28] The available bilayer T_ms for the PCs are therefore given in Table 1 and used to approximate PC interfacial film transition temperatures where these values are given.

The ordering of a series of symmetric chain PC layers adsorbed at similar interfacial concentrations at the CCl_4−D_2O interface was determined by VSFS as a function of diacyl chain length. As shown in Figure 3, the calculated CH_3-SS/CH_2-SS peak area ratio is nearly constant or slightly decreasing for DLPC (C_{12}/C_{12}) through DPPC (C_{16}/C_{16}), followed by a sharp increase in chain ordering as previously noted for DSPC (C_{18}/C_{18}) in Figure 2c. An abrupt increase in chain ordering from relatively disordered DPPC, $T_m = 41$ °C,[27] to very well ordered DSPC, $T_m = 55$ °C,[27] by the addition of only two methylene units per chain may indicate a distinct difference in phase below the respective main transition temperatures, which will be discussed further. Walker et al.[24] have made similar measurements on symmetric PC monolayers prepared at the CCl_4−D_2O interface by a different method, namely, transformation from aqueous liposomes heated to above the respective T_ms during adsorption to promote formation of a condensed monolayer and then cooled passively to room temperature. Those results are similar for DLPC (C_{12}/C_{12}) through DPPC (C_{16}/C_{16}) where the CH_3-SS/CH_2-SS ratio shows a slight decrease with chain length at the CCl_4−D_2O interface. However, in contrast to our theses a significant change in chain ordering for DSPC as compared to DPPC was not observed,[24] a difference that we attribute to differences in sample preparation technique. In heating the sample cell to promote complete monolayer formation (as verified by surface pressure measurements), which is very slow for liposomes in the lower temperature gel phase, the solubility of aqueous and CCl_4 phases in each other is increased, causing

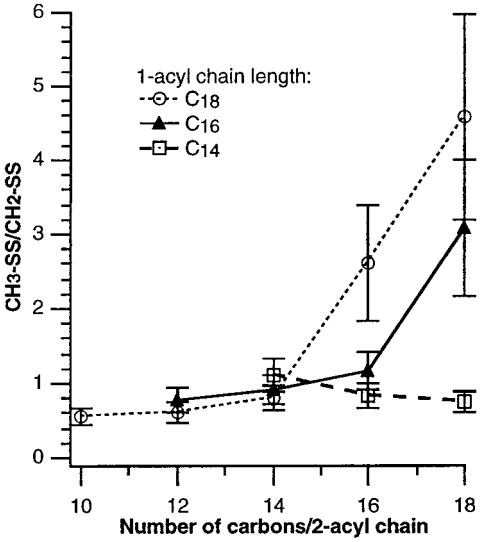

Figure 4. Peak area ratios for sn-1-stearoyl (C_{18} (○)), *sn*-1-palmitoyl (C_{16} (▲)), and *sn*-1-myristoyl (C_{14} (□)) PCs are shown as a function of 2-acyl chain length in number of carbon atoms.

molecules to move across the liquid−liquid interface in both directions. On allowing the sample cell to then cool to room temperature after the monolayer has formed, the opposite process occurs. It is likely that these changes in temperature indirectly disrupt the interfacial layer and prevent formation of a well-ordered DSPC layer in those studies. Excluding DLPC, which is above T_m at room temperature, interfacial adsorption below T_m using the technique described in this work has been shown to result in more ordered layers than those produced on adsorption above T_m.[29] The 55 Å^2 per PC molecule estimated from surface pressure measurements by Walker et al.[24] for adsorption at the CCl_4−water interface above T_m also indicates that, despite the high final surface pressures obtained in these measurements that would otherwise indicate formation of a close-packed monolayer, the PCs may be in either a liquid-expanded or phase coexistence region of the isotherm.[30] The results are consistent with electrochemical measurements reported by Kakiuchi et al.[31,32] for symmetric chain PCs adsorbed from nitrobenzene to the polarized nitrobenzene−water interface. Monolayers of adsorbed DSPC (C_{18}/C_{18}) and the longer chain PCs were thought to be in a less permeable liquid-condensed state, while the shorter chain PCs were more disordered and permeable.[31,32] The shorter chain PCs also occupy a much larger area per molecule in those studies than the C_{18} and longer chain PCs as deduced from surface pressure measurements.[32]

Peak area ratios calculated from VSFS measurements on interfacial layers of 1-stearoyl-2-capryl-*sn*-glycero-3-PC (SCPC; C_{18}/C_{10}), 1-stearoyl-2-lauroyl-*sn*-glycero-3-PC (SLPC; C_{18}/C_{12}), 1-stearoyl-2-myristoyl-*sn*-glycero-3-PC (SMPC; C_{18}/C_{14}), 1-stearoyl-2-palmitoyl-*sn*-glycero-3-PC (SPPC; C_{18}/C_{16}), and DSPC (C_{18}/C_{18}) adsorbed at room temperature to the liquid−liquid interface are given in Table 1 and plotted as a function of 2-acyl chain length in Figure 4. CH_3-SS/CH_2-SS peak ratios less than 1 were obtained for SCPC, SLPC, and SMPC, with SPPC being significantly more ordered and DSPC most ordered of the series. The difference in chain length, or chain mismatch, between the sn-1 and sn-2 acyl chains of the PC molecules clearly influences the chain packing arrangement. The mismatched portion of the longer hydrocarbon chains might be expected to have greater disorder proportional to the degree of mismatch resulting from reduced chain−chain interactions within a layer, consistent with

our observations. In bilayers, differences in the length of the two PC hydrocarbon chains, and particularly the mismatch between them, are thought to produce different degrees of interdigitation with resulting differences in ordering of the hydrocarbon chains.[11] In the same series SCPC (C_{18}/C_{10}), SLPC (C_{18}/C_{12}), SMPC (C_{18}/C_{14}), SPPC (C_{18}/C_{16}), and DSPC (C_{18}/C_{18}) each in the gel state below their respective T_ms, Raman studies suggested that the least ordered bilayer was SMPC.[11] SCPC and SLPC are thought to form mixed interdigitated bilayers, DSPC forms a noninterdigitated bilayer, and SPPC likely forms a partially interdigitated bilayer, all of which are reasonably well ordered.[11] SMPC, because of its intermediate degree of chain mismatch, can form neither a partially interdigitated nor a mixed interdigitated layer structure and is therefore the most disordered.[11] Consistent with our VSFS data, we might expect a monolayer, alone or as part of a multilayer structure, in the absence of an interdigitated opposing monolayer, to exhibit average ordering of the hydrocarbon chains, which is more directly a function of differences in chain length.

In Figure 4, an increase in chain ordering with chain length is also observed for the more symmetric *sn*-1-palmitoyl (C_{16}) PCs, PSPC (C_{16}/C_{18}), being significantly more ordered than 1-palmitoyl-2-lauroyl-*sn*-glycero-3-PC (PLPC; C_{16}/C_{12}), 1-palmitoyl-2-myristoyl-*sn*-glycero-3-PC (PMPC; C_{16}/C_{14}), and symmetric chain DPPC (C_{16}/C_{16}). The effective chain mismatch of DPPC may actually be greater than that for asymmetric PSPC due to the conformation of the PC backbone, as will be discussed below. The *sn*-1-myristoyl (C_{14}) PCs show slightly decreased ordering with increasing sn-2 chain length for films that are all fairly disordered, possibly as a combined effect of a shorter effective chain length and differences in chain mismatch.

In bilayers, chain mismatch has been quantified in a parameter ΔC/CL, in which $\Delta C = |n_1 - n_2 + 1.5|$ is the mismatch, in number of carbon−carbon bond lengths, between the sn-1 chain with n_1 carbon atoms and the sn-2 chain with n_2 carbon atoms.[11] The number 1.5 comes from the chain mismatch thought to be present in a symmetric chain PC (i.e., $n_1 = n_2$) in which the sn-2 chain extends an estimated 1.5 carbon−carbon bond lengths, or approximately 1.8 Å, less than the sn-1 chain into the hydrophobic bilayer interior.[11] CL is the length in number of carbon−carbon bonds of the longer of the two hydrocarbon chains, ($n_1 - 1$) or ($n_2 - 2.5$).[11] We initially assume in this analysis that the backbone conformation for PCs adsorbed at an oil−water interface is comparable to that for bilayers giving a 1.5 carbon−carbon bond length mismatch for the symmetric chain PCs. The CH_3-SS/CH_2-SS ratio is shown vs calculated chain mismatch, ΔC/CL, in Figure 5 for the various PCs. The results suggest that the most disordered films in the *sn*-1-stearoyl (C_{18}) series have a ΔC/CL greater than 0.3. A clear increase in hydrocarbon chain ordering is observed for SPPC (C_{18}/C_{16}) and DSPC (C_{18}/C_{18}), which have progressively lower values of the chain mismatch parameter. This is consistent with the surface pressure measurements of Ali et al.[13] for room-temperature *sn*-1-stearoyl PC monolayers at the air−water interface, in which smaller molecular areas were observed for the more symmetric (i.e., longer sn-2 acyl chain) molecules with lower chain mismatch at "membranelike" surface pressures, which are thought to correspond to approximately 30 mN/m.[33] PSPC (C_{16}/C_{18}), which has a lower calculated chain mismatch than DPPC (C_{16}/C_{16}) as previously mentioned, is far better ordered than any of the other *sn*-1-palmitoyl (C_{16}) PCs at the CCl_4-D_2O interface, including DPPC. This is again consistent with results from the air−water interface in which saturated *sn*-1-palmitoyl PCs with the sn-2 acyl chain 16 or more carbons in length have

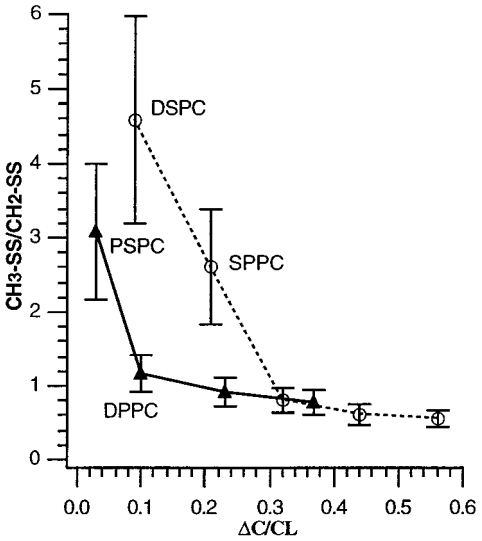

Figure 5. Hydrocarbon chain ordering, as indicated by the CH_3-SS/CH_2-SS peak area ratio calculated from VSFS measurements, as a function of the chain mismatch parameter, ΔC/CL for *sn*-1-stearoyl (C_{18} (○)) and *sn*-1-palmitoyl (C_{16} (▲)) PCs.

smaller molecular areas indicative of a more tightly packed layer.[12] It is interesting that despite the different calculated chain mismatch for PC isomers having the same two chains (e.g., C_{16}/C_{18} vs C_{18}/C_{16}), the chain ordering as deduced from VSFS does not seem to depend on the position, sn-1 or sn-2, to which the longer acyl chain is bound. Although a larger number of samples would be necessary to better define this trend, it is possible that the 1.5 carbon−carbon bond length chain mismatch deduced for bilayer systems of symmetric PCs[11] is not appropriate for PCs adsorbed at a CCl_4-D_2O interface. Unfortunately, a better estimate of this parameter is not available. Chain mismatch is, however, a useful and simple means to approximate the molecular chain asymmetry.

Ordering of PCs and other surfactants adsorbed at an oil−water interface is not generally expected to exhibit the same trends as at an air−water interface. Surface pressure vs area isotherms, especially at the lower molecular surface densities, are expanded at the oil−water as compared to the air−water interface, most likely due to hydrocarbon chain solvation by the oil phase.[30] Experimental investigations involving VSFS measurements of symmetric chain PC monolayers prepared in a different way from those in these investigations have indicated a decrease in hydrocarbon chain ordering with increasing chain length at the liquid−liquid interface.[24] Complimentary measurements at the air−water interface show an opposite trend.[24] However, isotherms at the two interfaces overlap at the higher surface pressures and similar molecular areas[12,30,34] where oil intercalating between PC hydrocarbon chains in more expanded states at the oil−water interface is presumably forced out.

From the preceding results, it is evident that the ordering of some PCs adsorbed at the CCl_4-D_2O interface is related to the degree of chain mismatch, but the formation of very well ordered layers with a majority of all-trans chain conformations was observed only for PCs with at least one stearoyl (C_{18}) chain, with the second chain being either stearoyl or palmitoyl (C_{16}). Comparison of the *sn*-1-stearoyl and *sn*-1-palmitoyl data of Figure 5 suggests that, as the effective length of the shorter PC hydrocarbon chain is increased, the individual PC monomers in the adsorbed film can maintain a well-ordered state with a greater degree of chain mismatch up to a point. It is also not likely to be coincidental that the three PCs that maintain well-ordered chains also have the highest (bilayer) T_ms, each at least

20 °C above room temperature, noting again that, although transition temperatures are generally reported for bilayers or aqueous dispersions, monolayer transition temperatures at the oil−water interface have been reported to be comparable.[28] A possible increase in temperature at the sample interface due to heating by the two incident laser beams must also be considered and will be discussed further, although normal variations in incident beam intensities between VSFS measurements did not appear to affect our results.

It has been reported that DPPC and DSPC dispersions in water undergo subtransitions from a crystalline to a gel state at 22 and 29 °C, respectively, following incubation at 0 °C for several days.[11,35] Onset of the subtransition on prolonged cooling is thought to correspond with a dehydration of the PC headgroup causing a compaction of the headgroup region and a subsequent stacking of the hydrocarbon chains.[36] On warming beyond the subtransition temperature, PC bilayers typically undergo a pretransition followed by a main transition with increasing area per PC molecule and an accompanying decrease in ordering of the hydrocarbon chains. At the gel-to-liquid crystalline phase transition temperature, or main transition, T_m, the strongest decrease in chain ordering occurs with chain melting.[37] In addition to symmetric chain PCs, many saturated, mixed chain PCs have also been reported to undergo subtransitions. In a series of PCs having a C_{18} chain in the sn-1 or sn-2 position and the chain in the other position varying between 10 and 18 (even numbers) carbons in length, PSPC, DSPC, and SPPC had the highest subtransition temperatures.[38] It is possible that the longer chain PCs adsorbed at the CCl_4-D_2O interface undergo a similar transition into a crystalline state below their respective subtransition temperatures, which would account for the large increase in hydrocarbon chain ordering observed at room temperature for DSPC as compared to DPPC. It has also been reported in some sources that racemic PC mixtures do not exhibit this crystalline-to-gel state subtransition,[39,40] while another study on DPPC revealed the presence of a DL-DPPC subtransition, only with a much lower excess enthalpy than that measured for L-DPPC.[36] If the longer chain L-PCs undergo a gel-to-crystalline subtransition to form the well-ordered layers observed, we would therefore expect a layer composed of a racemic mixture of the same long-chain PC to be less well ordered, consistent with the lack of a crystalline phase or the presence of a less stable low-temperature phase with a lesser degree of chain ordering.

Figure 6a shows the spectrum obtained by VSFS for DL-DSPC adsorbed at the CCl_4-D_2O interface by the same method of preparation used for other samples. It is clear from the very large CH_2-SS peak near 2850 cm^{-1} that this interfacially adsorbed layer formed by the racemic DSPC mixture is extremely disordered with respect to the hydrocarbon chains. The calculated CH_3-SS/CH_2-SS area ratio for this sample is 0.51 ± 0.22. It should also be noted that only a scant layer was formed at the liquid−liquid interface for this sample (i.e., the interface meniscus was not substantially reduced by addition of the phospholipid). However, using higher bulk aqueous phospholipid concentrations and/or longer adsorption periods up to 5 days, DL-DSPC did eventually form very well-ordered layers at the CCl_4-D_2O interface, as evidenced in the spectrum shown in Figure 6b. The calculated CH_3-SS/CH_2-SS peak area ratio of 4.55 ± 1.36 indicates that DL-DSPC becomes at least as well-ordered as L-DSPC allowing sufficient time. These observations suggest that, although both L-DSPC and DL-DSPC adsorbed at the CCl_4-D_2O interface do form crystalline phases as evidenced by VSFS of the hydrocarbon chains, differences in the rate of monolayer formation are apparent. Especially for condensed assemblies, the same packing arrangements found in monolayers, multilayers, and bilayers of PC L-enantomers are not likely to be geometrically favorable in the mixture. Consistent with our results, it has also been suggested that differences in molecule chirality are more likely to be reflected in packing of the polar headgroup region rather than of the hydrophobic chains.[39]

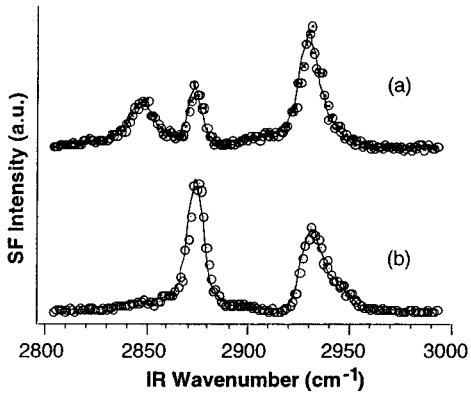

Figure 6. Measured SSP sum frequency intensity vs IR wavenumber for adsorbed layers of the racemic DSPC mixture. Representative spectra are shown for (trace a) an incomplete layer prepared by the standard method and (trace b) a tightly packed layer observed using either higher bulk PC concentrations and/or longer equilibration times.

As mentioned previously in the discussion, some degree of heating of the interfacial region being sampled by VSFS is likely such that the actual temperature of the sample spot being probed may be somewhat above room temperature. Referring to the T_ms given for the various PCs in Table 1, the layers that appeared by VSFS measurements to be well-ordered have main transition temperatures of 44 °C and higher. Of the remaining disordered PCs, DPPC has the highest T_m at 41 °C. Assuming the amount of heating is the same for all samples studied, if laser heating of the sample spot is responsible for a transition from the gel to liquid crystalline phase in samples that would otherwise be in a well-ordered gel state at room temperature, we could estimate a surface temperature of between 41 and 44 °C. In addition to expected differences between bilayers and PCs adsorbed at an oil−water interface related to environmental influences of the liquid−liquid interface, which are not well understood, this is one possible explanation for the lack of correlation between ordering of the adsorbed PC chains and whether T_m for the particular PC is above or below room temperature. The potential significance of this surface heating will be explored in future work.

The observation that DL-DSPC forms well-ordered layers less readily than does L-DSPC argues in favor of a gel-to-crystalline subtransition occurring in the long-chain PCs studied to induce well-ordered nearly all-trans chain conformations in adsorbed DSPC, SPPC, and PSPC at room temperature. As previously mentioned, subtransitions have been observed typically in enantomerically pure saturated PCs after low-temperature incubation near 0 °C for several days to months.[35,38] It is therefore quite intriguing to have possibly obtained crystalline layer formation in less than 24 h at 22 °C. A possible explanation for this phenomenon is the unusual "icelike"organization of water molecules, which has been experimentally observed at an oil−water interface.[41] It is possible that the nature of the CCl_4−water interface may serve to partially dehydrate the PC headgroups promoting formation of the subgel crystalline phase. It is noteworthy that emulsion particles, modeling plasma lipoproteins, which were stabilized by long-chain symmetric PCs

are metabolized in vivo at a much reduced rate compared to emulsions stabilized by a more fluid unsaturated PC closer to the natural composition.[5] The well-ordered layers of the symmetric, long-chain PCs may therefore overstabilize the emulsion, forming a barrier to normal metabolic processes.

Conclusions

We have reported original observations of differences in hydrocarbon chain ordering among a series of saturated symmetric and asymmetric chain PCs adsorbed at a CCl_4-D_2O interface that depend on the length of the shorter hydrocarbon chain and degree of hydrocarbon chain length mismatch within the PC molecule. Three of the PCs studied, specifically SPPC (C_{18}/C_{16}), DSPC (C_{18}/C_{18}), and PSPC (C_{16}/C_{18}), formed extremely well-ordered layers with primarily all-trans chain conformations at the liquid−liquid interface by room-temperature adsorption from the aqueous phase. Highly asymmetric PCs showed relatively disordered chains, as might be expected from the reduced chain−chain interactions among the mismatched portions of the longer chains. The shorter chain PCs (<16 carbons/chain) were also relatively disordered. The greater disorder seen in the shorter chain PCs, irrespective of chain mismatch, is a likely consequence of reduced chain−chain interactions over a smaller chain length.

It is noteworthy that the main differences measured in adsorbed PC film organization could not be predicted based on the respective gel-to-liquid crystalline (bilayer) phase transition temperatures. Disordered chains were observed both for PCs above and below their respective T_ms at room temperature. The most pronounced differences in organization (i.e., the well-ordered long-chain PCs) may result from interfacial layer subtransitions. The apparent ability of the oil−water interface to nucleate the formation of adsorbed crystalline PC layers in the absence of extended low-temperature equilibration points to differences between bilayer and adsorbed oil−water PC assemblies distinct from chain solvation effects. Further interface-specific characterizations using VSFS will help to shed light on additional potentially unique features of PCs and other natural surface-active molecules adsorbed at liquid−liquid interfaces.

Acknowledgment. The authors thank Dr. R. A. Walker for helpful discussions and T. E. Hannon for preliminary studies with the asymmetric PCs. Financial support from the National Science Foundation (CHE 9725751) and the Office of Naval Research is gratefully acknowledged.

References and Notes

(1) Prince, L. M. In *Biological Horizons in Surface Science*; Prince, L. M., Sears, D. F., Eds.; Academic Press: New York, 1973; p 353.
(2) Handa, T.; Saito, H.; Miyajima, K. *Biochemistry* **1990**, *29*, 2884.
(3) Miller, K. W.; Small, D. M. In *Plasma Lipoproteins*; Gotto, A. M. J., Ed.; Elsevier: New York, 1987; Vol. 14, p 1.
(4) Schumaker, V.; Lembertas, A. In *Molecular Genetics of Coronary Artery Disease. Candidate Genes and Processes in Atherosclerosis*; Lusis, A. J., Rotter, J. I., Sparkes, R. S., Eds.; Karger: New York, 1992; Vol. 14, p 98.
(5) Redgrave, T. G.; Rakic, V.; Mortimer, B.-C.; Mamo, J. C. L. *Biochim. Biophys. Acta* **1992**, *1126*, 65.
(6) Davis, S. S.; Hadgraft, J.; Palin, K. J. In *Encyclopedia of Emulsion Technology*; Becher, P., Ed.; Marcel Dekker, Inc.: New York, 1985; Vol. 2, p 159.
(7) Krog, N. J.; Riisom, T. H.; Larsson, K. In *Encyclopedia of Emulsion Technology*; Becher, P., Ed.; Marcel Dekker, Inc.: New York, 1985; Vol. 2, p 321.
(8) Ogino, K.; Onishi, M. *J. Colloid Interface Sci.* **1981**, *83*, 18.
(9) Goerke, J. *Biochim. Biophys. Acta* **1974**, *344*, 241.
(10) Yeagle, P., Ed. *The Structure of Biological Membranes*; CRC Press, Boca Raton, 1992.
(11) Huang, C.; Mason, J. T. *Biochim. Biophys. Acta* **1986**, *864*, 423.
(12) Evans, R. W.; Williams, M. A.; Tinoco, J. *Biochem. J.* **1987**, *245*, 455.
(13) Ali, S.; Smaby, J. M.; Momsen, M. M.; Brockman, H. L.; Brown, R. E. *Biophys. J.* **1998**, *74*, 338.
(14) Bell, G. R.; Bain, C. D.; Ward, R. N. *J. Chem. Soc., Faraday Trans.* **1996**, *92*, 515.
(15) Shen, Y. R. *Surf. Sci.* **1994**, *299/300*, 551.
(16) Eisenthal, K. B. *Chem. Rev.* **1996**, *96*, 1343.
(17) Conboy, J. C.; Messmer, M. C.; Richmond, G. L. *J. Phys. Chem. B* **1997**, *101*, 6724.
(18) Du, Q.; Superfine, R.; Freysz, E.; Shen, Y. R. *Phys. Rev. Lett.* **1993**, *70*, 2313.
(19) Bloembergen, N.; Lee, C. H. *Phys. Rev. Lett.* **1967**, *19*, 835.
(20) Bloembergen, N.; Simon, H. J.; Lee, C. H. *Phys. Rev.* **1969**, *181*, 1261.
(21) Walker, R. A.; Conboy, J. C.; Richmond, G. L. *Langmuir* **1997**, *13*, 3070.
(22) Shchipunov, Y. A.; Kolpakov, A. F. *Adv. Colloid Interface Sci.* **1991**, *35*, 31.
(23) Conboy, J. C.; Messmer, M. C.; Richmond, G. L. *J. Phys. Chem.* **1996**, *100*, 7617.
(24) Walker, R. A.; Gruetzmacher, J. A.; Richmond, G. L. *J. Am. Chem. Soc.* **1998**, *120*, 6991.
(25) Snyder, R. G.; Strauss, H. L.; Elliger, C. A. *J. Phys. Chem.* **1982**, *86*, 5145.
(26) Guyot-Sionnest, P.; Hunt, J. H.; Shen, Y. R. *Phys. Rev. Lett.* **1987**, *59*, 1597.
(27) Marsh, D. *CRC Handbook of Lipid Bilayers*; CRC Press, Inc., Boston, 1990.
(28) Small, D. M.; Steiner, J. W.; Derksen, A.; Clark, S. B. *Biophys. J.* **1988**, *53*, 211.
(29) Smiley, B. L.; Walker, R. A.; Gragson, D. E.; Hannon, T. E.; Richmond, G. L. *SPIE* **1998**, *3273*, 134.
(30) Mingins, J.; Taylor, J. A. G.; Pethica, B. A.; Jackson, C. M.; Yue, B. Y. T. *J. Am. Chem. Soc., Faraday Trans. 1* **1982**, *78*, 323.
(31) Kakiuchi, T.; Kotani, M.; Noguchi, J.; Nakanishi, M.; Senda, M. *J. Colloid Interface Sci.* **1992**, *149*, 279.
(32) Kakiuchi, T. In *Liquid−Liquid Interfaces: Theory and Methods*; Volkov, A. G., Deamer, D. W., Eds.; CRC Press: Boca Raton, 1996; p 317.
(33) Blume, A. *Biochim. Biophys. Acta* **1979**, *557*, 32.
(34) Alexander, A. E.; Teorell, T. *Trans. Faraday Soc.* **1939**, *35*, 727.
(35) Finegold, L.; Singer, M. A. *Chem. Phys. Lipids* **1984**, *35*, 291.
(36) Kodama, M.; Hashigami, H.; Seki, S. *Biochim. Biophys. Acta* **1985**, *814*, 300.
(37) Lewis, R. N. A. H.; McElhaney, R. N. In *The Structure of Biological Membranes*; Yeagle, P., Ed.; CRC Press: Boca Raton, 1992; p 73.
(38) Mattai, J.; Sripada, P. K.; Shipley, G. G. *Biochemistry* **1987**, *26*, 3287.
(39) Boyanov, A. I.; Tenchov, B. G.; Koynova, R. D.; Koumanov, K. S. *Biochim. Biophys. Acta* **1983**, *732*, 711.
(40) Koynova, R.; Tenchov, B. G.; Todinova, S.; Quinn, P. J. *Biophys. J.* **1995**, *68*, 2370.
(41) Gragson, D. E.; Richmond, G. L. *Langmuir* **1997**, *13*, 4804.